

Estimation of the Surface Roughness in Cylindrical Plunge Grinding Based on Material Removal Model

Yulun Chi^{**}, Aili Ge^{*} and Haolin Li^{*}

Keywords : cylindrical plunge grinding, surface roughness estimation, material removal rate model, power signal

ABSTRACT

As an important variable of the grinding quality, the surface roughness is a variable often used to describe the performance of the finished part as well as to evaluate the competitiveness of the overall grinding system. Hence, the estimation of surface roughness can cater to the requirements of performance evaluation. A new surface roughness model for multi-infeed cylindrical plunge grinding based on the material removal rate is established by using the monitoring power signal. It shows that steady-state surface roughness and the change in surface roughness are related separately to the grinding wheel wear and the material removal rate, the relationships of which are investigated. A series of experiments was performed to verify that estimation algorithm of surface roughness is effective and repeatable in grinding process control. The results demonstrated that the roughness model is valuable for designing process parameters to achieve the grinding quality index and the process optimization.

INTRODUCTION

The reliability of mechanical components, especially for high-strength applications, is often critically dependent upon the quality of the surface produced by grinding.

Paper Received November, 2016. Revised March, 2019. Accepted July, 2019. Author for Correspondence: Yulun Chi

** Associate Professor, Shanghai University for Science and Technology, Shanghai 200093, P.R.China.*

*** Graduate Student, Shanghai University for Science and Technology, Shanghai 200093, P.R.China*

The general grinding process can be described as a finishing process to achieve material removal and desired surface finish. In several common types of grinding, Karpuschewski et al. (2000)¹ reviewed that cylindrical plunge grinding has been widely used to machine precision shaft parts and surface roughness is one of the most important quality attributes to be obtained on the ground part. However, the actual determination the values of grinding parameters to acquire the desired surface roughness are always accompanied by difficulties because of the machining complex process and a large number of affecting factors². So, the determinations made by engineers are based only on their experience and expertise but also on conventions regarding the phenomena that take place during processing³. To overcome these difficulties, the researchers have proposed models that tried to establish the cause and influence relationships between various factors and desired product surface roughness. Many theoretical methods of surface roughness evaluation, as reported in the literature, have been proposed to estimate the surface roughness during grinding process⁴⁻⁷. In analytical models, Hecker et al. (2003)⁴ proposed that the surface roughness has been characterized by the description of the microstructure of the grinding wheel in both one and two dimensions, which take the grain distance, the width of cutting edge and the grain diameter into account. Stepien et al. (2009)⁵ developed the random arrangement of the grain vertices at the wheel active surface and the process of shaping the ground surface roughness, the probability of contact as well as the undeformed chip thickness are also described in the grinding zone. Agarwal et al. (2015)⁶ proposed a new analytical surface roughness model developed on the basis of stochastic nature of the grinding process, governed mainly by the random geometry and the random distribution of cutting edges on the wheel surface having random grain protrusion heights. And it is validated by the experimental results of AISI 4340 steel in surface grinding. Despite these have advanced in the understanding and modeling of the grinding processes, these models developed to date are seldom

utilized in industrial applications. In empirical methods, the surface roughness model is always shown as a function of kinematic conditions, such as the one presented by Malkin et al (2002) ⁷, which has had more success in the industry because they do not need the effort of material and surface wheel characterizations. However, the elastic deflection of the grinding contact zone and the actual material removal rate are not considered in these models. Many parameters and the grinding wheel properties are just lumped into empirical constants.

With the development of monitoring technology, the methods related to estimations of grinding wheel performance and grinding quality using model coefficients are also presented. Jiang et al. (2014) ⁸ reported a monitoring of the acoustic emission (AE) model used to calculate the on-line time constant of the dwell period and to estimate the workpiece grinding quality by predicting the minimum dwell time, and the proposed material can be easily used to removal models ⁹⁻¹⁰ during the dwell time satisfying constraints for industrial application. However, the model forms don't take the grinding wheel wear process into account and its applicability is limited. According to the grinding material removal mechanism, CHI et al. (2016) ¹¹⁻¹² presented that the general grinding material removal rate model was established by using the monitoring power signal. According to the improved power signal model, an attempt has been made to develop a surface roughness estimation model with considering the wheel wear process for cylindrical plunge grinding process in this paper. A relationship between surface roughness and the wheel wear process has been established with the material removal rate. A simple and easy-to-use generalized roughness models have been developed and presented by using the monitoring power signal. At last, the estimation model is verified using experimental data from the surface grinding of C45 steel with aluminium oxide abrasive.

ESTIMATION OF CYLINDRICAL PLUNGE GRINDING SURFACE ROUGHNESS

A new surface roughness model for multi-infeed cylindrical plunge grinding based on the material removal rate is established by using the monitoring power signal, which is introduced by the following work.

Model of power signals

In earlier work by CHI et al. (2016) ¹¹, a model of the power signal during a multi-infeed plunge grinding cycle was built for the monitoring of material removal. In the proposed model, the curves

of power signal during the grinding process can be simulated by:

$$P = \frac{k_c k_p v_s}{k_m n_w} (\dot{u}_n + (\dot{u}_{n-1} - \dot{u}_n) e^{-\frac{t-t_{n-1}}{\tau}} + \dots + (\dot{u}_1 - \dot{u}_2) e^{-\frac{t-t_1}{\tau}} + (\dot{u}_0 - \dot{u}_1) e^{-\frac{t-t_0}{\tau}}) \quad (1)$$

where, k_p is the coefficient of power, v_s is the grinding wheel speed, n is the order of the infeed stage, \dot{u}_n is the commanded infeed rate of the n th infeed stage, t_n represents the infeed time during the previous n stages, k_c is the stiffness of the grinding action to relate the real depth of the cut to the normal grinding force, n_w is the workpiece rotational speed, k_m is the proportionality coefficient of the normal force and the tangential force and τ is the time constant.

According to Eq. (1), the proportionality coefficient $\frac{k_c k_p}{k_m}$ and the time constant τ can be easily determined by examining the steady-state power P' as well as the rate of power change \dot{P} reached in one time constant τ (τ is generally on the order of one second in precision grinding) ¹³.

$$P = P' \approx \frac{k_c k_p v_s \dot{u}_n}{k_m n_w} \equiv K_s \quad (t - t_{n-1} \gg \tau) \quad , \quad (2)$$

$$\dot{P} = \frac{k_c k_p v_s}{k_m n_w} (\dot{u}_n - \dot{u}_{n-1}) e^{-1} \equiv \frac{K_s \left[\left(1 - \frac{u_{n-1}}{u_n}\right) e^{-1} \right]}{\tau} \quad (t - t_{n-1} = \tau, t - t_{n-2} \gg \tau) \quad , \quad (3)$$

Eqs. (2) and (3) can be applied to grinding power data to periodically update the empirical values of τ and K_s . Once τ and K_s are known, the removed material may be quickly predicted by solving for the grinding contact time t_{grind} using equation (4):

$$t_{grind} = \tau \left(\frac{(\dot{u}_{n-1} - \dot{u}_n) e^{-\frac{t_{grind}-t_{n-1}}{\tau}} + \dots + (\dot{u}_1 - \dot{u}_2) e^{-\frac{t_{grind}-t_1}{\tau}} + (\dot{u}_0 - \dot{u}_1) e^{-\frac{t_{grind}-t_0}{\tau}}}{\dot{u}_n \left(\frac{P}{K_s} - 1 \right)} \right) \quad , \quad (4)$$

where, the time constant τ can be estimated using the experimental power signal data.

Plunge grinding material removal rate model

At the start of cylindrical plunge grinding, $\dot{u}_0 = 0$ and $t_0 = 0$. Accordingly, the general relationship model for different infeed stages is established, and the prediction of the material removed and material removal rate are performed using Eqs. (5) and (6).

$$r_n^{grind}(t) = \dot{u}_n (t_{grind} - \tau) + (\dot{u}_{n-1} - \dot{u}_n) (t_{n-1} - \tau e^{-\frac{t_{grind}-t_{n-1}}{\tau}}) + \dots + (\dot{u}_1 - \dot{u}_2) (t_1 - \tau e^{-\frac{t_{grind}-t_1}{\tau}}) + (\dot{u}_0 - \dot{u}_1) (t_0 - \tau e^{-\frac{t_{grind}-t_0}{\tau}}) \quad , \quad (5)$$

$$\dot{r}_n^{grind}(t) = \dot{u}_n + (\dot{u}_{n-1} - \dot{u}_n)e^{-\frac{t_{grind} - t_{n-1}}{\tau}} + \dots + (\dot{u}_1 - \dot{u}_2)e^{-\frac{t_{grind} - t_1}{\tau}} + (\dot{u}_0 - \dot{u}_1)e^{-\frac{t_{grind} - t_0}{\tau}}, \quad (6)$$

If $t - t_{n-2} \gg \tau$, then Eqs. (5) and (6) can be simplified by:

$$\dot{r}_n^{grind}(t) = \dot{u}_n(t_{grind} - \tau) + (\dot{u}_{n-1} - \dot{u}_n)(t_{n-1} - \tau)e^{-\frac{t_{grind} - t_{n-1}}{\tau}} + (\dot{u}_{n-2} - \dot{u}_{n-1})t_{n-2} + \dots + (\dot{u}_1 - \dot{u}_2)t_1 + (\dot{u}_0 - \dot{u}_1)t_0, \quad (7)$$

$$\dot{r}_n^{grind}(t) = \dot{u}_n + (\dot{u}_{n-1} - \dot{u}_n)e^{-\frac{t_{grind} - t_{n-1}}{\tau}}. \quad (8)$$

Compared with similar work done by Marsh et al. (2008)¹⁴, the general model uses all of the elastic deformation of the previous infeed stages in the current infeed stage simulation, especially when the stage ($t - t_{n-1}$ to $t - t_0$) cannot be neglected. Because the model does not neglect the effectiveness of the previous infeed stages, it is more accurate to simulate and predict the multi-infeed cylindrical plunge grinding. The following parts demonstrate the utility of the model in the surface roughness estimation of cylindrical plunge grinding.

Model of power signals

Hasegawa et al. (1974)¹⁵ presented that the 'ideal' surface profile has been generated by computer simulation for measured wheel profiles or statistical models thereof. As shown in Fig.1, each subsequent wheel profile passing a particular location on the workpiece is considered to remove material in its path left behind by previous profiles and to improve the surface roughness progressively. For computational simplicity, the outer points on successive wheel profiles are assumed to protrude to the same height. And, the soothing effect is followed an approximate relationship of the form by Bhateja et al. (1977)¹⁶.

$$R_a = \frac{R_0}{i} + R_{k,\infty}, \quad (9)$$

Where, i is the number of wheel profiles, R_0 and $R_{k,\infty}$ are empirical constants. It is assumed that the number of wheel topography profiles contributing to the workpiece profile would depend on the grinding parameters, the number of profiles can be expressed as:

$$i = \frac{v_s (R_i d_s)^{1/2}}{v_w L}, \quad (10)$$

where, L is the spacing between successive active cutting points or profiles, R_i is the arc length of contact for a wheel depth of cut, v_s is the grinding workpiece speed and d_s is the grinding wheel diameter.

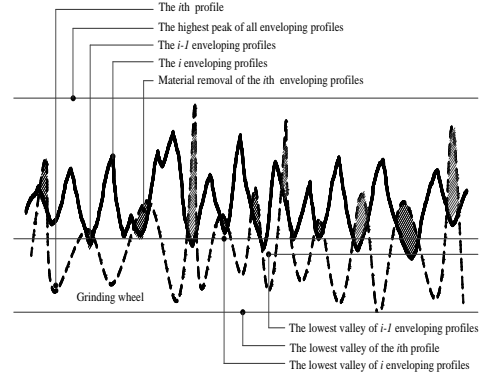


Fig.1 Ideal workpiece envelope profile across the grinding direction by Bhateja et al. (1977)¹⁵.

Assuming that the ratio between R_t and R_a is fixed (i.e. $R_t = mR_a$). According to the Eqs. (9) and (10), the surface roughness, which is arithmetic mean deviation of contour of grinding workpiece, can be approximated by Malkin et al. (2002)⁷:

$$R_a = \left(\frac{R_0}{m^{0.5}} \right) \left(\frac{v_w L}{v_s d_e^{0.5}} \right)^{0.8} + R_{k,\infty}, \quad (11)$$

Where, m is the proportionality coefficient, d_e is the equivalent diameter of the wheel and L is the spacing between successive active cutting points or profiles, which can be shown as:

$$L = \sqrt{ad_e}, \quad (12)$$

Where the instantaneous depth of the grinding depth a is related to the actual feed velocity \dot{r}_n and the workpiece velocity ω_w according to:

$$a = \frac{\dot{r}_n}{\omega_w}. \quad (13)$$

The surface roughness R_a obtained by combining Eqs. (11), (12) and (13) can be expressed by:

$$R_a = \left(\frac{R_0}{m^{0.5}} \right) \left(\frac{\left(\frac{d_e}{2} v_w \dot{r}_n \right)^{0.5}}{v_s} \right)^{0.8} + R_{k,\infty}. \quad (14)$$

As shown in Eq. (14), the grinding surface roughness R_a is corresponded to the material removal rate \dot{r}_n and the empirical constant $R_{k,\infty}$. It is apparent from actual operations that the grinding wheel grains wear effect the constant value $R_{k,\infty}$ directly. So, the estimation of surface roughness R_a should be considered for the material removal rate \dot{r}_n and the grinding wheel wear condition

Estimation model of cylindrical plunge grinding surface roughness

As an important variable of the grinding quality, the surface roughness R_a is always used in monitoring and optimizing of cylindrical plunge grinding. As theoretical analysis shown in Fig.1, the generation of surface roughness is directly related to the wheel topography and the operating parameters. By using the monitoring signal, it is very important to estimate the grinding workpiece surface roughness online. In this following part, a new practical model is proposed to estimate the surface roughness R_a by considering the grinding wheel wear process and the material removal rate.

The surface roughness in terms of grinding wheel wear

During the spark-out stage, the surface roughness R_a tends towards the 'steady state' value $R_{k,\infty}$ when $t_{grind} \gg t_{n-1}$. With continuous grinding cycles, the progressive wears in the wheel topography affect the 'steady state' surface roughness $R_{k,\infty}$. The change of the surface roughness $R_{k,\infty}$ having been studied from the very moment the grinding wheel is freshly dressed until it wears. A close relationship between the 'steady state' surface roughness $R_{k,\infty}$ and the wheel wear process has been found by malkin et al. (2002)⁷. The changed behavior of $R_{k,\infty}$ from $R_{a,0}$ towards $R_{a,\infty}$ can be show as:

$$\frac{R_{k,\infty} - R_{a,\infty}}{R_{a,0} - R_{a,\infty}} = \exp\left(\frac{V_w'}{V_0'}\right), \quad (15)$$

where, $R_{a,0}$, $R_{a,\infty}$ and V_0' are constants, V_w' is the accumulated metal removal per unit with after dressing which can be expressed by:

$$V_w' = kr_n, \quad (16)$$

where, k is the number of grinding cycles or parts, r_n is the material removal for every grinding cycle. So, the 'steady state' surface roughness $R_{k,\infty}$ can be described by instituting Eq. (16) into Eq. (15).

$$R_{k,\infty} = R_{a,\infty} + (R_{a,0} - R_{a,\infty}) \exp\left(-\frac{kr_n}{V_0'}\right), \quad (17)$$

where, r_n can be acquired by using grinding parameters and power signal, the coefficients $R_{a,0}$, $R_{a,\infty}$ and V_0' can be calculated from the actual measured surface roughness data. As above analysis, the $R_{k,\infty}$ value highly depends on the grinding wheel wear condition.

The surface roughness in terms of material removal rate.

For one grinding cycle, the grinding workpiece surface roughness R_a value is greatly decided by the spark-out time. Before the surface roughness of the workpiece R_a reaches a steady value $R_{n,\infty}$, the relationship between the change in the surface roughness ΔR_k and the material removal rate \dot{r}_n should be established to estimate the surface roughness R_a more effectively. The change in the surface roughness of workpiece ΔR_k can be expressed by Eq. (18) which is related to the material removal rate \dot{r}_n directly.

$$\Delta R_k = \left(\frac{R_0}{m^{0.5}}\right) \left(\frac{\left(\frac{d_e}{2} v_w \dot{r}_n\right)^{0.5}}{v_s}\right)^{0.8}. \quad (18)$$

The material removal rate \dot{r}_n can be acquired from Eq. (6). Substituting Eq. (6) into Eq. (18), the change in the surface roughness of workpiece ΔR_k can be shown as:

$$\Delta R_{k-\max} = \left(\frac{R_0}{m^{0.5}}\right) \left(\frac{\left(\frac{d_e}{2} v_w (\dot{u}_{n-1} + (\dot{u}_{n-2} - \dot{u}_{n-1})e^{-\frac{t_{n-1}-t_{n-2}}{\tau}} + \dots + (\dot{u}_0 - \dot{u}_1)e^{-\frac{t_{n-1}-t_0}{\tau}})\right)^{0.4}}{v_s^{0.8}}\right)^{0.4}. \quad (19)$$

At the beginning of the spark-out stage ($t_{grind} = t_{n-1}$), the change in the surface roughness of spark-out stage reaches a maximum value $\Delta R_{k-\max}$ which can be expressed by:

$$\Delta R_{k-\max} = \left(\frac{R_0}{m^{0.5}}\right) \left(\frac{\left(\frac{d_e}{2} v_w (\dot{u}_{n-1} + (\dot{u}_{n-2} - \dot{u}_{n-1})e^{-\frac{t_{n-1}-t_{n-2}}{\tau}} + \dots + (\dot{u}_0 - \dot{u}_1)e^{-\frac{t_{n-1}-t_0}{\tau}})\right)^{0.4}}{v_s^{0.8}}\right)^{0.4}. \quad (20)$$

When $t_{grind} \gg t_{n-1}$, $\dot{r}_n(t) = 0$, the change in the surface roughness of spark-out stage ΔR_k is closed to zero which can be shown as:

$$\Delta R_k \approx 0. \quad (21)$$

From above Eq. (17) and (20), the change in the surface roughness of workpiece ΔR_k is related to the material removal rate \dot{r}_n . Especially during the spark-out stage, the change in the surface roughness of workpiece is close to zero when $\dot{r}_n(t) = 0$. It means that the surface roughness of the workpiece R_a reaches a steady state ($R_{k,\infty}$) when $t_{grind} \gg t_{n-1}$.

According to Eq. (15) and (20), the grinding surface roughness can be estimated from the grinding parameters and power signals. In addition, the amount of material which should be removed per

wheel dressing, or the number of parts per dressing, can be calculated by the change limit of the 'steady state' surface roughness $R_{k,\infty}$.

Experimental setup

A series of experiments was performed using a CNC cylindrical grinding machine to verify that estimation algorithm of surface roughness is effective and repeatable in grinding process control using power signal. As is shown in Fig.2, the STUDER K-C33 multi-purpose CNC cylindrical grinding machine equipped with an air-bearing workpiece spindle is used to process the workpiece which was installed by using two centers. The grinding parameters of the experimental wheel and the workpiece are shown in Table.1

Table.1 The parameters of the grinding wheel and workpiece

Parameter	Property
Workpiece material	C45
Wheel material	Vitrified aluminum oxide
Workpiece dimension(mm)	$\Phi 50(\text{diameter}) \times 200(\text{length})$
Wheel dimension(mm)	$\Phi 460(\text{diameter}) \times 60(\text{width}) \times \Phi 220(\text{bore})$
Workpiece speed(r/min)	120
Wheel speed(m/s)	36
Wheel spindle power (kW)	20
Coolant	7% Emulsion Syntilo 9930

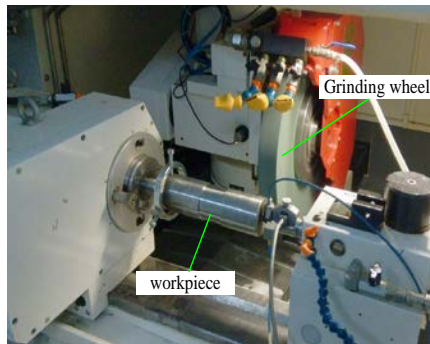


Fig.2 Grinding machine setup

In this experiment, the power signal of wheel electric spindle is used to study the plunge grinding surface roughness. The electric spindle power is measured using a power sensor LOAD CONTROL PH-3A installed in a machine tool electrical cabinet. The power sensor is designed to sense 3 phase power and works on both fixed frequency and variable frequency power. It is used as a standalone transducer with an analog output (0-10 Volts). The power signal is filtered and digitised using a DATAQ INSTRUMENTS DI-148U data acquisition card.

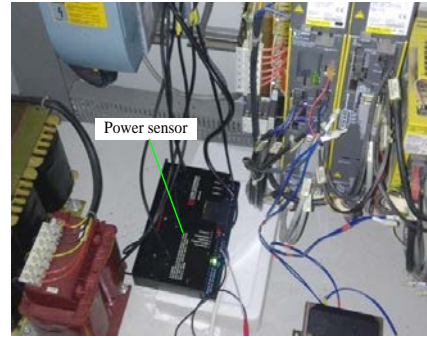


Fig.3 Power sensor install

The average surface roughness for grinded workpiece was measured by using a laser-check 6212B scattered laser light instrument across the grinding direction at different three positions. As is shown in Fig.4, laser-check non-contact technology provides immediate surface testing without damage to workpiece surfaces. It is easy to set up and use. In high volume surface grinding operations, laser-check 6212B can quickly and easily measure product surfaces, ensuring process and quality control.

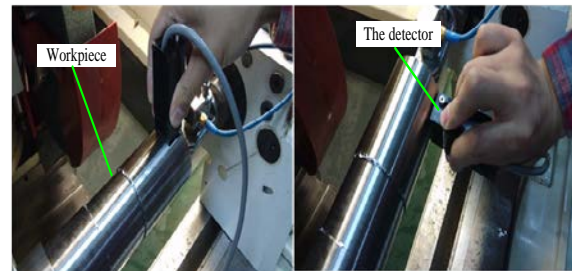


Fig.4 Workpiece roughness measurement

Results and discussion

This discussion is divided into four parts based on the experimental work. First, the experimental data were collected to study the relationship between the steady surface roughness and the grinding wheel wear. Its results are further proved by the wheel surface microscope measurement. Second, a lot of tests were performed to study the change in grinding surface roughness related to different spark-out time (material removal rate) by using the power signal. Third, the surface roughness estimated by the model, including the change in surface roughness and the steady surface roughness, is compared with the experiment measurement results. It appears to be reasonably close agreement between the experimental and estimated results. Finally, an estimation of the spark-out time and the grinding wheel performance using different surface roughness limitations is presented. The results demonstrated that the roughness model is valuable for designing process parameters to achieve the grinding quality index and the process optimization.

Estimation of roughness $R_{k,\infty}$ in terms of grinding wheel wear

Nineteen continuous grinding experiments, with a feed rate of $12\mu\text{m/s}$ after the wheel dressing, were performed to study the steady grinding surface roughness in terms of grinding wheel wear. In each whole grinding cycle, the spark-out stage lasted 12 s, as is shown in table.2, and the workpiece three positions surface roughness $R_{k,\infty}$ was measured by using the method of Fig.4.

Table.2 The experiment grinding parameters

Infeed allowance (mm)	Infeed speed ($\mu\text{m/s}$)	Spark-out time (s)	Grinding cycles
0.1	12	12	19

As is shown in Fig.5 (a), the steady roughness results of three positions and Fig.5 (b) the average roughness results, are increasing with the grinding cycles at the beginning from zero to eight. In this period, the grinding wheel wears out gradually with more and more material removal. Hence this causes the grinding surface roughness increasing, which is agreement with the Fig.1 analysis results. When the grinding cycles reach eight, the grinding wheel wears completely, and there is no obvious change for the grinding surface roughness again. The explanation of this phenomenon is that the grinding wheel has been wearing out seriously, and the grinding surface roughness reaching balance and not increasing any more.

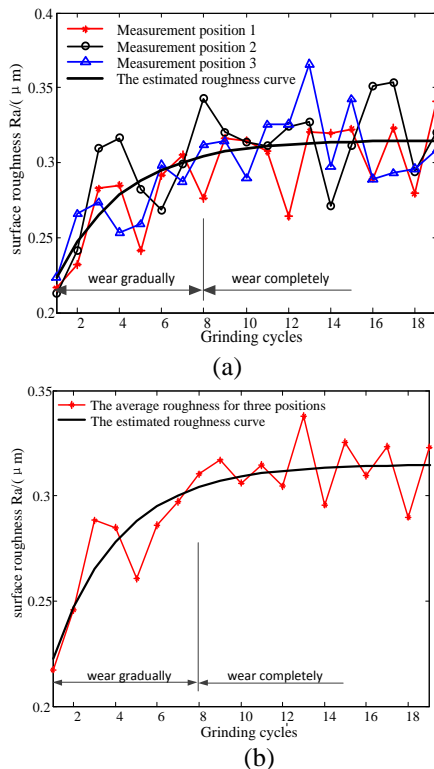


Fig.5 Grinding surface roughness results: (a) the roughness results of three positions, (b) the average roughness

Furthermore, the wheel surface measurement experiments by using KENYCE VHX 3000, with 220×100 times, were performed to verify the above analysis relationship between the grinding surface roughness $R_{k,\infty}$ and the grinding wheel wear process. As is shown in Fig.6 (a), it shows clear surface of the grinding wheel after dressing. With consecutive grinding cycles, the wheel surface wears more and more seriously as shown in Fig.6 (b), Fig.6 (c) and Fig.6 (d). It also indicates that the wheel surface deterioration in the process featured by the abrasive wear and wheel loading. Therefore, it is possible to evaluate the wheel performance by using the grinding surface roughness $R_{k,\infty}$ to control dressing automatically to assure the grinding wheel performance well.

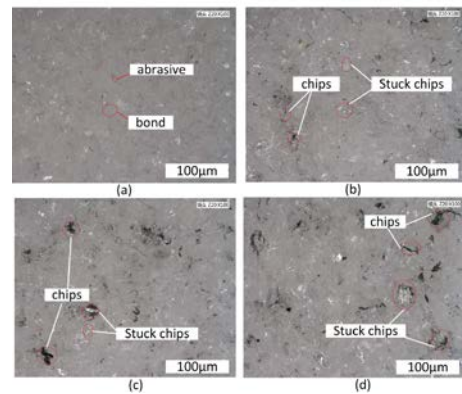


Fig.6 The wheel surface change with grinding cycles: (a) the wheel surface after dressing, (b) the wheel surface after the first cycle, (c) the wheel surface after the fourth cycle, (d) the wheel surface after the eighth cycle

The validity of the model Eq. (17) is assessed through a comparison between the estimated value and measured value of the steady surface roughness within the predefined parameters, and the coefficients $R_{a,\infty}$, $R_{0,\infty}$ and r_n/V_0 can be determined

by the measured roughness results in Fig.5, where $R_{a,\infty}$ is 0.3152, $R_{0,\infty}$ is 0.18998 and r_n/V_0 is 0.3072.

Fig.5 (a) and Fig.5 (b) show the comparison of the estimated and the measured surface roughness results. It can be seen that the estimated surface roughness also changes obviously when the grinding cycles exceed eight times, and is almost consistent with the measured results.

In the real plunge grinding process, there is some error between the estimated and the measured surface roughness which may be caused by the uncontrollable grinding factors, such as coolant force,

thermal error structure system vibration and so on. According to the operator's experience, the estimated roughness results are acceptable to be used to estimate the grinding surface roughness.

Estimation of roughness ΔR_k in terms of material removal rate

In order to study the change in grinding surface roughness ΔR_k related to different spark-out time, a lot of tests with an infeed speed of $12\mu\text{m/s}$, were performed with monitoring power signal by using different operation parameters as shown in Table.3. To avoid the influences of wheel wear, the automated dressing process is performed for every group grinding parameters. The surface roughness of the workpiece at each spark-out time is measured by the method of Fig.3.

Table.3 The experiment grinding parameters

Exp.no	Infeed allowance (mm)	Infeed speed ($\mu\text{m/s}$)	Spark-out time (s)
1	0.1	12	0
2	0.1	12	1
3	0.1	12	2
4	0.1	12	3
5	0.1	12	4
6	0.1	12	5
7	0.1	12	6
8	0.1	12	7
9	0.1	12	8
10	0.1	12	9
11	0.1	12	10

Fig.8 shows the change trend of the surface roughness in the grinding experiments while the spark-out time is changed from 0 to 10 s. The surface roughness decreases with the increasing spark-out time at the beginning, and is steady at around $0.32\mu\text{m}$ after the spark-out time reaching 4 s. As mentioned above, the measured surface roughness R_a can be divided into two parts which are the change in surface roughness of workpiece ΔR_k and the steady surface roughness $R_{k,\infty}$. This means that the minimum spark-out time obtained by the surface roughness in experiments is 4s and the minimum surface roughness $R_{k,\infty}$ is $0.32\mu\text{m}$ at an infeed speed of $12\mu\text{m/s}$. In this section, to estimate the change in surface roughness ΔR_k in terms of spark-out time, the measured surface roughness R_a should

minus the steady roughness $R_{k,\infty}$, then the concrete results are shown in Fig.7.

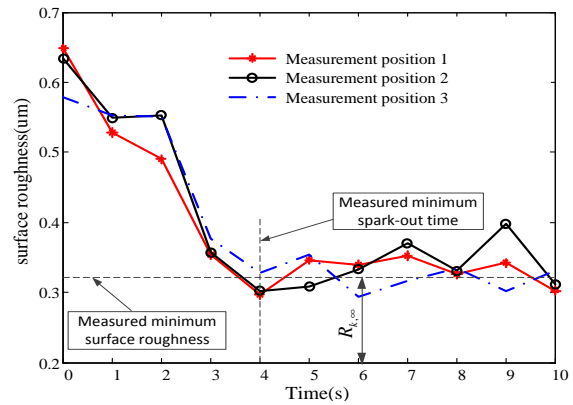


Fig.7 The measured surface roughness at different spark-out time

To verify the model of Eq. (19), the material removal rate \dot{r}_n can be determined by the monitoring power signal. Gao et al. (1999)¹⁷ proposed that the observed value of the coefficient K_s is directly related to the steady state of the grinding power, while the time constant τ is a function of the system compliance and material removal rates. A flow chart for the determination of these coefficients is introduced by CHI et al. (2016). The power curve was obtained using Eq. (1) with the calculated coefficients. As is shown in Fig. 8, the prediction of the power curve was similar to the measured power signal, which proves the validity of the calculated material removal rate \dot{r}_n .

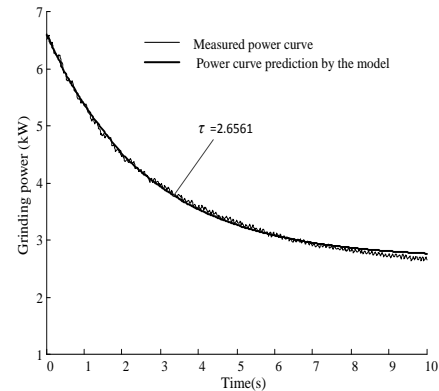


Fig.8 Comparison between the predicted and measured power curve

Substituting the predicted material removal rate \dot{r}_n into Eq. (19), the change in surface roughness ΔR_k can be calculated as shown in Fig.9. The three positions measurement roughness results, which minus the steady roughness $R_{k,\infty}$, are compared with the theoretical model results. It can be seen from the

Fig.9 that both the model estimated and the experimental results have similar decreasing trends until reaching a steady state value close to zero. There is a good agreement between the two. When the spark-out time exceeds 4s, there is also not obvious change for both the predicted and experimental roughness curve.

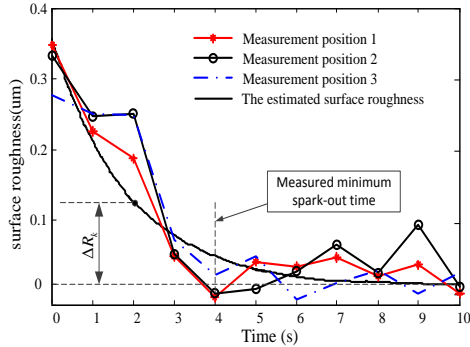


Fig.9 The estimated surface roughness ΔR_k compared with the measured results

Estimation of roughness R_a in spark-out stage

The surface roughness model R_a described above, which is easily affected by the spark-out time and the wheel condition, includes the change in surface roughness of workpiece ΔR_k and the steady surface roughness $R_{k,\infty}$. Therefore, the model R_a can be used to estimate the surface roughness by considering those two parts.

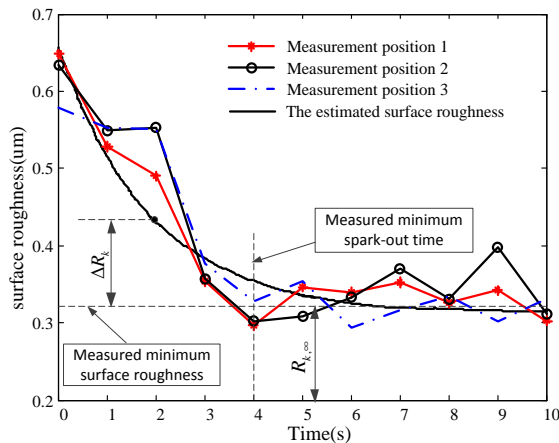


Fig.10 Comparison between the estimated and measured roughness

As it is shown in Fig.10, there appears to be reasonably close agreement between the experimental and estimated results. It can be observed that, at the spark-out time (0 ~ 4 s), the changes on the value of the surface roughness is significant due to the high material removal rate. After the spark-out time 4 s, the surface roughness changes little. This is because that there is less change for the material removal rate

during the spark-out time (4 ~ 8 s), and the wheel grains participated in material removing are not increasing obviously. However, the grinding wheel conditions play a major role in the value of the steady surface roughness $R_{k,\infty}$ according to the section 4.1. Therefore, the roughness model can be used to evaluate the wheel condition, the redressing process and the minimum spark-out time to assure the workpiece surface quality.

The improvement of grinding efficiency and quality

A proportional relation among the wheel wear (the grinding cycles), the material removal rate (the spark-out time) and the surface roughness, was derived from the above analytical analysis. The threshold value of surface roughness $R_{a\lim}$ for every cycle is very important to define the minimum spark-out time $t_{spark-min}$ to improve the plunge grinding efficiency. At the same time, the threshold value of steady surface roughness $R_{k,\infty\lim}$ can be set up to decide the maximum grinding cycles k_{max} after that the grinding wheel should be redressed to keep its microscopic surface sharp enough to assure the process quality. As it is shown in Fig.11, based on the model estimation roughness R_a , the minimum spark-out time $t_{spark-min}$ and the grinding cycles k_{max} before redressing can be known when the $R_{a\lim}$ and $R_{k,\infty\lim}$ are set according to the actual grinding process.

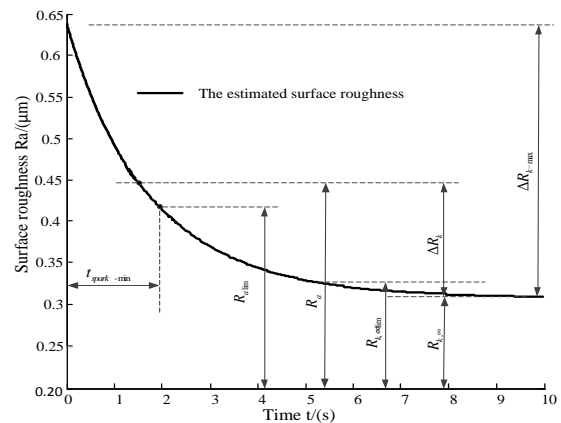


Fig.11 The minimum spark-out time through estimated roughness

As explained in Fig.11, different surface roughness thresholds $R_{k,\infty\lim}$ and $R_{a\lim}$ are selected to generate the minimum spark-out time $t_{spark-min}$. And the maximum grinding cycles k_{max} before the grinding wheel redressing is shown in Table 4.

Table.4 The minimum spark-out time and maximum grinding cycles

Exp.no	$\Delta R_{k-\max}$	$R_{a\lim}$	$R_{k,\infty\lim}$	$t_{\text{spark-min}} \text{ (s)}$	k_{\max}
1	0.3631	0.5324	0.32	1.0	8
2	0.3631	0.4819	0.32	1.5	8
3	0.3631	0.4433	0.32	2.0	8
4	0.3631	0.4138	0.32	2.5	8
5	0.3631	0.3913	0.32	3.0	8
6	0.3631	0.3741	0.32	3.5	8
7	0.3631	0.3609	0.32	4.0	8
8	0.3631	0.3508	0.32	4.5	8
9	0.3631	0.3408	0.31	4.5	7
10	0.3631	0.3308	0.30	4.5	6
11	0.3631	0.3208	0.29	4.5	5
12	0.3631	0.3108	0.28	4.5	4
13	0.3631	0.3008	0.27	4.5	3
14	0.3631	0.2908	0.26	4.5	2
15	0.3631	0.2708	0.24	4.5	1

As it can be seen, the surface roughness $R_{a\lim}$ can be acquired with increasing the spark-out time, and the surface roughness $R_{k,\infty\lim}$ can be finished by redressing the grinding wheel within k_{\max} grinding cycles. Such as, more spark-out time (from 1 s to 4.5 s) is required to get less grinding surface roughness $R_{a\lim}$ (from 0.5324 μm to 0.3508 μm), and the maximum grinding cycles (from 8 to 1) before the grinding wheel redressing present same trends with the surface roughness $R_{k,\infty\lim}$ (from 0.32 μm to 0.24 μm). The results were also experimentally proved in a lot of tests. This indicates that the grinding workpiece efficiency and quality can be controlled with different surface roughness limitation.

The results show that the above model can be used to design grinding process parameters to achieve the workpiece quality index and the process optimization. The major advantage of using the models is that these models maintain the same functional forms regardless of different plunge grinding workpiece-wheel combinations, and hence can be readily applied to various grinding set-ups by determining their coefficients through a small number of designed experiments. This is very important for the actual operator to find the solution to achieve the process requirement through the material removal mechanism and the surface roughness model.

Conclusions

For cylindrical plunge grinding process, simple and easy-to-use generalized roughness models with the material removal rate have been developed and presented in this paper. The following conclusion can be drawn:

(1) As an important variable of the grinding quality, the new surface roughness model for multi-infeed cylindrical plunge grinding based on the material removal rate, is established by using the monitoring

power signal. The roughness model considers both the grinding wheel wear process and the material removal rate. Furthermore, it has also been shown that the steady-state surface roughness and the change in surface roughness are related separately with the grinding wheel wear and the material removal rate, which relationships are investigated. It means that the new roughness model can be used to design process parameters to achieve the grinding quality index.

(2) A series of experiments were performed to verify that estimation algorithm of surface roughness is effective and repeatable in grinding process control by using power signal. In this experiment, laser-check 6212B is used quickly and easily to measure workpiece grinding surface roughness, and the power signal of wheel electric spindle is used to study the plunge grinding surface roughness. Furthermore, the wheel surface measurement experiments, using the KENYCE VHX 3000 microscope, were used to measure the wheel surface topography directly to verify the theoretical analysis.

(3) Based on the theoretical analysis, the experimental data was collected to study the relationship between the steady surface roughness and the grinding wheel wear. Then, a lot of tests were performed to study the change in grinding surface roughness related to different spark-out time (material removal rate). It can be found both the model estimated and the experimental results have same decreasing trends until reaching a steady state value, and the estimated method is proved.

(4) Finally, the surface roughness estimated by the model, including the change in surface roughness and the steady surface roughness, is compared with the experiment measurement results. And, an estimation of the spark-out time and the grinding wheel performance using different surface roughness limitations is presented. The results demonstrated that the roughness model is valuable for designing process parameters to achieve the grinding quality index and the process optimization.

The surface roughness model with the material removal rate presents obvious advantages in including the terms of the effect of wheel wear for the actual operator to find the solution to achieve the process requirement based on the power signal. Another important aspect is that it can be used to automatically optimise the grinding parameters in terms of the total grinding time or total grinding cost. The grinding optimisation process will be studied in detail in future work.

ACKNOWLEDGEMENT

This work was financially supported by the National Science and Technology Support Program (2013ZX04008-011)

REFERENCES

- Agarwal, S., Kharea, S.K., 2015. *Predictive modeling of surface roughness in grinding*. Procedia. CIRP. 31: 375-380.
- Bhateja, C.P., "An Enveloping Profile Approach for the Generation of Ground Surface Texture," *Ann. CIRP.*, Vol.25, No.1, pp: 333, 1977.
- Chen, X., Rowe, W.B., Mills, B., Allanson, D.R., "Analysis and simulation of the grinding process. Part III. Comparison with experiment," *Int. J. Mach. Tools. Manuf.*, Vol.36, No.8, pp: 897-906, 1996.
- CHI, Y., LI, H., "A general material removal model for multi-infeed internal plunge grinding by using power signal," *J. Chin. Soc. Mechn. Eng.*, Vol. 37, No.4: 359-365, 2016.
- CHI, Y., LI, H., Chen, X., "In-Process Monitoring and Analysis of Bearing Outer Race Way Grinding based on the Power Signal," *Proc. IMechE. Part B: J Engineering Manufacture*, Vol.231, No.14: 2622-2635, 2017.
- Gao, Y., Jones, B., "Fast time constant estimation for plunge grinding process control," *Int. J. Mach. Tools. Manuf.*, Vol.39, No.1, pp: 143-156, 1999.
- Hasegawa, M., "Statistical Analysis for the Generating Mechanism of Ground Surface Roughness," *Wear.*, Vol.29, No.1, pp:31-39, 1974.
- Hecker, R.L., Steven, Y.L., "Predictive modeling of surface roughness in grinding," *Int. J. Mach. Tools. Manuf.*, Vol.43, No.8, pp: 755-761, 2003.
- Jiang, C., Li, H., Mai, Y., Guo, D., "Material removal monitoring in precision cylindrical plunge grinding using acoustic emission signal," *Proc. IMechE. Part C: Journal of Mechanical Engineering Science*, Vol.228, No.4, pp: 715-722, 2014.
- Jiang, C., Song, Q., Guo, D., Li, H., "Estimation algorithm of minimum dwell time in precision cylindrical plunge grinding using acoustic emission signal," *Int. J. Precis. Eng. Man.*, Vol.15, No.4, pp: 601-607, 2014.
- Karpuschewski, B., Wehmeier, M., Inasaki, I., "Grinding monitoring system based on power and acoustic emission sensors [J]," *Ann. CIRP.*, Vol.49, No.1, pp: 235-240, 2003.
- Malkin, S., "Grinding Technology: Theory and Application of Machining with Abrasives," *Northeastern University Press*, pp: 130-153, 2002.
- Manu Dogra, Vishal S. Sharma, Jasminder Singh Dureja, Environment-friendly technological advancements to enhance the sustainability in surface grinding – A review. *Journal of Cleaner Production*, 2018, 197:218-231.
- Marsh, E.R., Moerlein, A.W., Deakyne, T.R.S., Doren, M.J.V., "In-process measurement of form error and force in cylindrical-plunge grinding," *Precis. Eng.*, Vol.32, No.4, pp: 348-352, 2008.
- Moerlein, A.W., Marsh, E.R., Deakyne, T.R.S., Vallance, R.R., "In-process force measurement for diameter control in precision cylindrical grinding," *Int. J. Adv. Manuf. Technol.*, Vol. 42, pp: 93-101, 2009.
- Satyarthi, M.K., Pandey, P.M., "Modeling of material removal rate in electric discharge grinding process," *International Journal of Machine Tools & Manufacture*, Vol.74, No.74, pp: 65-73, 2013.
- Stepien, P., "A probabilistic model of the grinding process," *Appl. Math. Model.*, Vol.33, No.10, pp: 3863-3884, 2009.
- Suting Chen, Rui Feng, Chuang Zhang, Yanyan Zhang. *Surface roughness measurement method based on multi-parameter modelling learning*. Measurement, 2018, 129: 664-676.

NOMENCLATURE

- a grinding depth
- d_e equivalent diameter of the wheel
- d_s grinding wheel diameter
- i number of wheel profiles
- k number of grinding cycles or parts
- k_c stiffness of the grinding action to relate the real depth of the cut to the normal grinding force
- k_p coefficient of power
- k_{nt} proportionality coefficient of the normal force and the tangential force
- k_{max} the maximum grinding cycles
- L the spacing between successive active cutting points or profiles
- m proportionality coefficient
- n order of the infeed stage
- n_w workpiece rotational speed

P' steady-state power
 \dot{P} the rate of power change
 R_a surface roughness
 $R_{k,\infty}$ the 'steady state' surface roughness
 $R_{n,\infty}$ the steady surface roughness value
 ΔR_k the relationship between the change in the surface roughness
 r_n material removal
 $\Delta R_{k,\max}$ the maximum surface roughness value
 $R_{a\lim}$ the threshold value of surface roughness
 $R_0, R_{k,\infty}$ empirical constants
 R_t the arc length of contact for a wheel depth of cut
 $R_{a,0}, R_{0,\infty}, R_{a,\infty}$ and V_0' the constants
 $R_{k,\infty\lim}$ the threshold value of steady surface roughness
 r_n^{grind} prediction of material removal
 \dot{r}_n the actual feed velocity
 t_n infeed time during the previous n stages
 $t_{spark-min}$ the minimum spark-out time
 t_{grind} grinding contact time
 \dot{u}_n commanded infeed rate of the n th infeed stage
 v_s grinding workpiece speed
 V_w' the accumulated metal removal per unit with after dressing
 v_s grinding wheel speed
 ω_w workpiece velocity
 V_w' the accumulated metal removal per unit with after

dressing
 v_s grinding wheel speed
 ω_w workpiece velocity

基於材料去除模型的外圓 切入式磨削表面粗糙度預 測

遲玉倫 葛愛麗 李郝林
 上海理工大學機械工程學院

摘 要

表面粗糙度作為磨削加工品質的一個重要指標，常用於評價產品零件性能以及整個磨削系統加工能力。因此，表面粗糙度預測可適用於系統性能評價的需求。本文利用監測功率信號建立了一種基於材料去除率的多進給外圓切入式磨削表面粗糙度模型。該模型表明穩態階段表面粗糙度變化分別與砂輪磨損和材料去除率有關，並研究了粗糙度與兩者之間的關係。最後，通過大量實驗驗證該表面粗糙度預測模型在磨削加工程式控制應用的有效性和可靠性。試驗結果表明該粗糙度預測模型對於優化磨削工藝參數和控制磨削加工品質具有重要意義。